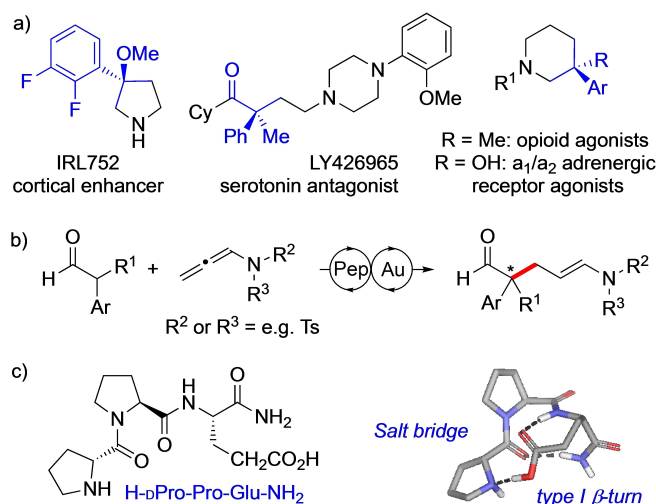


# Synergistic Peptide and Gold Catalysis: Enantioselective Addition of Branched Aldehydes to Allenamides

 Leo D. M. Nicholls<sup>[a]</sup> and Helma Wennemers<sup>\*[a]</sup>

**Abstract:** The combination of a peptide catalyst and a gold catalyst is presented for enantioselective addition reactions between branched aldehydes and allenamides. The two catalysts act in concert to provide  $\gamma,\delta$ -enamides bearing a fully substituted, benzylic stereogenic center – a structural motif common in many natural products and therapeutically active compounds – with good yields and enantioselectivities. The reaction tolerates a variety of alkyl and alkoxy substituted aldehydes and the products can be elaborated into several chiral building blocks bearing either 1,4- or 1,5- functional group relationships. Mechanistic studies showed that the conformational features of the peptide are important for both the catalytic efficiency and stereochemistry, while a balance of acid/base additives is key for ensuring formation of the desired product over undesired side reactions.



**Figure 1.** a) Selected therapeutically active compounds containing fully substituted benzylic stereogenic centers. b) The enantioselective addition of  $\alpha$ -branched aldehydes to allenamides. c) Tripeptide catalyst H-dPro-Pro-Glu-NH<sub>2</sub> and its conformation.

Fully substituted, benzylic stereogenic centers are important building blocks of many natural products and biologically active compounds (Figure 1a).<sup>[1]</sup> These structural motifs have become the target of a variety of synthetic methodologies.<sup>[2–4]</sup> Among them, an attractive approach relies on amine catalyzed reactions between branched aldehydes and suitable carbon-based electrophiles, which proceed through reactive enamine intermediates.<sup>[5,6]</sup> In recent years, the combination of a metal catalyst with an amine catalyst has expanded the scope to include otherwise unreactive electrophiles.<sup>[7,8]</sup> Interesting electrophiles to be used in these types of reactions are allenamides,<sup>[9]</sup> which can act as synthetically versatile C-2 or C-3 synthons through synthetic elaboration of the enamide moiety formed after C–C bond formation (Figure 1b).<sup>[10]</sup> Recently, two elegant studies by Mascareñas/López and González showcased the feasibility of reactions between branched aldehydes and

allenamides catalyzed by prolinol silyl ethers and Au-based catalysts.<sup>[11]</sup> These reports also pointed out that dual catalysis is challenging since the organocatalyst and the metal catalyst must act in concert and not interfere with each other.<sup>[11,12]</sup> We reasoned that amine-based catalysts, in which the amino group is shielded and therefore less prone to interact with the metal catalyst, may offer advantages in this reaction.

Our group developed the peptide H-dPro-Pro-Glu-NH<sub>2</sub>, which is a highly efficient and stereoselective organocatalyst for C–C bond formations that rely on the formation of enamine intermediates.<sup>[13,14]</sup> Detailed NMR spectroscopic analyses revealed that this peptide adopts a stable ground state conformation, in which the amine moiety forms a salt bridge with the glutamic acid side chain (Figure 1c).<sup>[15]</sup> We envisioned that this intramolecular coordination would disfavor non-productive interactions between the peptide and the metal center and that as a result, peptides of the type H-dPro-Pro-Xaa would be efficient catalysts for the targeted transformations.

Herein, we report the stereoselective addition of branched aldehydes to allenamides, catalyzed by a synergistic combination of peptide and gold catalysts. The reaction proceeds under mild conditions, tolerates a broad range of alkyl-aryl and alkoxy-aryl aldehydes and provides the addition products with good to excellent enantioselectivities. The aldehyde-enamide products proved to be synthetically versatile for further elaboration into chiral building blocks including diols, lactones

[a] Dr. L. D. M. Nicholls, Prof. H. Wennemers

Laboratory of Organic Chemistry  
ETH Zürich

Vladimir-Prelog-Weg 3, 8093 Zürich (Switzerland)

E-mail: Helma.Wennemers@org.chem.ethz.ch

Supporting information for this article is available on the WWW under <https://doi.org/10.1002/chem.202103197>

© 2021 The Authors. Chemistry - A European Journal published by Wiley-VCH GmbH. This is an open access article under the terms of the Creative Commons Attribution Non-Commercial NoDerivs License, which permits use and distribution in any medium, provided the original work is properly cited, the use is non-commercial and no modifications or adaptations are made.

and piperidines. We also show that the conformational properties of the tripeptide catalyst and a fine balance between the reaction components (peptide, gold, acid, and base) are key for the efficiency of the reaction.

We started our investigations to evaluate the duality of peptide and metal catalysts using the reaction between 2-phenylpropanal (**1a**) and allenylsulfonamide **2a** as a model reaction (Table 1). Firstly, we tested a range of different Cu, Au, Pd, Rh, and Ir complexes known to activate allenamides and/or allenes and used H-DPro-Pro-Glu-NH<sub>2</sub> (**4a**) as peptide catalyst (Table 1, entries 1–5, Table S1). Many of the tested metal-complexes did not allow access to the desired addition product or only in poor yields. Furthermore, dimerization of **2a** to allenamide dimer **6** was observed.<sup>[16,17]</sup> These findings underscored the challenge of identifying metal complexes that are compatible with amine-based catalysts. The best results were obtained with gold carbene complex **5a**<sup>[18,19]</sup> that in combination with peptide **4a** provided a promising conversion of 62% to  $\gamma,\delta$ -enamido aldehyde **3a** with an enantioselectivity of 47% (Table 1, entry 2). N-methyl morpholine (NMM) was included as

a base since the trifluoroacetic acid (TFA) salt of the peptide was used.

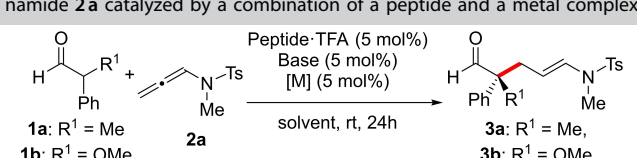
Variations of the peptide catalyst revealed that the stereochemistry, the CO<sub>2</sub>H group and its position as well as the length of the side chain of the C-terminal amino acid are important for high yield and selectivity (Table 1, entries 2, 6, 7; Table S2). The DLL stereochemistry and the glutamic acid residue (peptide **4a**), features that allow for the intramolecular salt bridge, provided the best results and the lowest amount of side products such as the allenamide dimer **6**. Installation of an alkyl chain at the C-terminus of the peptide (**4d**) improved the enantioselectivity of the reaction further (Table 1, entry 8). It is possible that the alkyl chain increases the local hydrophobicity and thereby stabilizes the salt bridge and improves the selectivity of the reaction.<sup>[20]</sup> Examination of other key reaction parameters revealed that the use of chloroform as solvent increased the enantioselectivity and an excess of the aldehyde improved the yield (Table 1, entries 9 and 10, Tables S5 and S6). TFA, the counterion of the peptide, proved to be important for the reactivity and enantioselectivity and better suited than other acids (e.g., benzoic acid, H<sub>2</sub>CICCO<sub>2</sub>H, Ph<sub>2</sub>P(O)OH; Table S7). Finally, a screen of different bases, including DBU, DABCO, and Et<sub>3</sub>N, identified that DMAP is slightly superior to NMM (Table 1, entry 11, Table S8). Under these optimized conditions,  $\gamma,\delta$ -ensulfonamide aldehyde **3a** was obtained in 80% yield with an enantioselectivity of 83%.

We then allowed aldehyde **1b**, substituted with a methoxy instead of a methyl group, to react with allenylsulfonamide **2a** and obtained the product with an enantioselectivity of 88% ee (Table 1, entry 12). This stereoselectivity could be further increased to 95% by using tripeptide **4e** that has an aspartic acid in place of a glutamic acid residue as well as through fine-tuning of the reaction conditions (aldehyde:allenamide = 1.5:1, 0.05 M, <sup>i</sup>Pr<sub>2</sub>NEt as base) (Table 1, entry 13; Tables S10–S16).

With optimized reaction conditions in hand, we proceeded to evaluate a scope of the reactions between allenamides and alkyl-aryl aldehydes (Scheme 1) and alkoxy-aryl aldehydes (Scheme 2). Pleasingly, the products from reactions with branched alkyl-aryl aldehydes were obtained with good yields and enantioselectivities (**3a**, **3c–3f**, 60–80% yield, 78–83% ee; Scheme 1). Even carbamate protecting groups (Boc and Alloc) at the nitrogen in the allenamine were tolerated and provided the enamide products **3g** and **3h** with comparable stereoselectivity. Branched allenylsulfonamides resulted in only traces of product (**3i**), most likely due to the increased steric requirement.

Also aldehydes bearing a methoxy group and different electron rich and electron poor aryl moieties at C<sup>α</sup> formed  $\gamma,\delta$ -ensulfonamide aldehydes with good yields (58–80%) and excellent enantioselectivities (90–95% ee) (**3b**, **3j–3l**; Scheme 2). Reactions with aldehydes bearing sterically more demanding alkoxy substituent proceeded with moderate to good yields but the high enantioselectivities were retained (**3m–3o**; Scheme 2).<sup>[21]</sup> Single crystals of the major enantiomer of **3b** suitable for X-Ray diffraction could be grown and revealed the absolute stereochemistry at the fully substituted stereogenic center to be (S).<sup>[22,23]</sup>

**Table 1.** Addition reaction between aldehydes **1a** and **1b** and allenylsulfonamide **2a** catalyzed by a combination of a peptide and a metal complex.



Peptide: **4a**: R<sup>2</sup> = CH<sub>2</sub>CO<sub>2</sub>H, R<sup>3</sup> = NH<sub>2</sub>  
**4b**: R<sup>2</sup> = CO<sub>2</sub>H, R<sup>3</sup> = NH<sub>2</sub>  
**4c**: R<sup>2</sup> = CONH<sub>2</sub>, R<sup>3</sup> = NH<sub>2</sub>  
**4d**: R<sup>2</sup> = CH<sub>2</sub>CO<sub>2</sub>H, R<sup>3</sup> = NHC<sub>12</sub>H<sub>25</sub>  
**4e**: R<sup>2</sup> = CO<sub>2</sub>H, R<sup>3</sup> = NHC<sub>12</sub>H<sub>25</sub>

[M]: **5a**: Au(MeCN) with Dipp, BF<sub>4</sub><sup>-</sup>  
**5b**: Au(MeCN) with tBu, tBu, Ph, SbF<sub>6</sub><sup>-</sup>  
**5c**: Cu(OTf)<sub>2</sub>/2•PPh<sub>3</sub>  
**5d**: Cu(CN)<sub>4</sub>BF<sub>4</sub>

allenamide dimer **6**

Entry	Aldehyde	Peptide	Base	Solvent	Conv. [%] <sup>[a]</sup>	ee [%] <sup>[b]</sup>
1	<b>1a</b>	<b>4a</b>	NMM	CH <sub>2</sub> Cl <sub>2</sub>	< 5	–
2	<b>1a</b>	<b>4a</b> , <b>5a</b>	NMM	CH <sub>2</sub> Cl <sub>2</sub>	62	47
3	<b>1a</b>	<b>4a</b> , <b>5b</b>	NMM	CH <sub>2</sub> Cl <sub>2</sub>	22	45
4	<b>1a</b>	<b>4a</b> , <b>5c</b>	NMM	CH <sub>2</sub> Cl <sub>2</sub>	< 5	–
5	<b>1a</b>	<b>4a</b> , <b>5d</b>	NMM	CH <sub>2</sub> Cl <sub>2</sub>	< 5	–
6	<b>1a</b>	<b>4b</b> , <b>5a</b>	NMM	CH <sub>2</sub> Cl <sub>2</sub>	43	34
7	<b>1a</b>	<b>4c</b> , <b>5a</b>	NMM	CH <sub>2</sub> Cl <sub>2</sub>	16	25
8	<b>1a</b>	<b>4d</b> , <b>5a</b>	NMM	CH <sub>2</sub> Cl <sub>2</sub>	59	69
9	<b>1a</b>	<b>4d</b> , <b>5a</b>	NMM	CHCl <sub>3</sub>	64	80
10 <sup>[c]</sup>	<b>1a</b>	<b>4d</b> , <b>5a</b>	NMM	CHCl <sub>3</sub>	81	79
11 <sup>[c]</sup>	<b>1a</b>	<b>4d</b> , <b>5a</b>	DMAP	CHCl <sub>3</sub>	(80)	83
12	<b>1b</b>	<b>4d</b> , <b>5a</b>	NMM	CHCl <sub>3</sub>	(80)	88
13 <sup>[d]</sup>	<b>1b</b>	<b>4e</b> , <b>5a</b>	<sup>i</sup> Pr <sub>2</sub> NEt	CHCl <sub>3</sub>	(80)	95

Unless otherwise stated, reactions were carried out using an equal stoichiometry of aldehyde **1a/1b** and allenylsulfonamide **2a** at a concentration of 0.2 M in CH<sub>2</sub>Cl<sub>2</sub>. [a] Conversion to **3a/3b** estimated by <sup>1</sup>H NMR spectroscopic analysis of the crude mixture using 1,3,5-trimethoxybenzene as internal standard. Yields in parentheses. [b] Enantiomeric excess determined by chiral stationary phase SFC. [c] 2 equiv. aldehyde used. [d] 1.5 equiv. aldehyde used, at 0.05 M. NMM = N-methylmorpholine, DMAP = 4-(dimethylamino)pyridine, Dipp = 1,6-diisopropylphenyl.



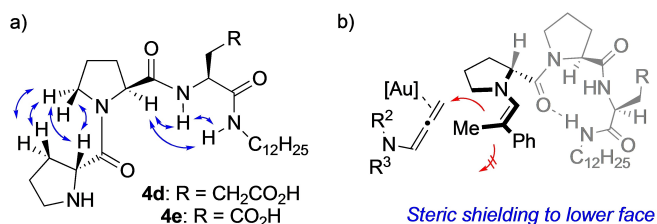


Figure 2. a) NOEs observed in the NMR spectra of peptides **4d** and **4e**. b) Stereochemical model of C–C bond formation.

three components in a 1:1:1 ratio and analysed the mixture by <sup>1</sup>H NMR spectroscopy. The spectrum shows one major set of signals relating to the peptide catalyst and two sets of signals in a ratio of ~10:1 relating to the gold catalyst (Figure 3). The chemical shifts of the signals relating to the peptide indicate that peptide **4d** exists in an equilibrium between the TFA-salt and the “desalted” form, a finding that was corroborated by a titration of the peptide-TFA salt with DMAP (Figure S5). The major set of signals for the gold species relates to Au-DMAP complex **13** and the minor set of signals to Au-TFA complex **14**. In addition, a small amount of the salt formed by DMAP and TFA is visible. These assignments were supported by comparison with authentic samples by <sup>1</sup>H and <sup>19</sup>F NMR spectroscopy and, in case of **13**, further confirmed by crystal structure analysis

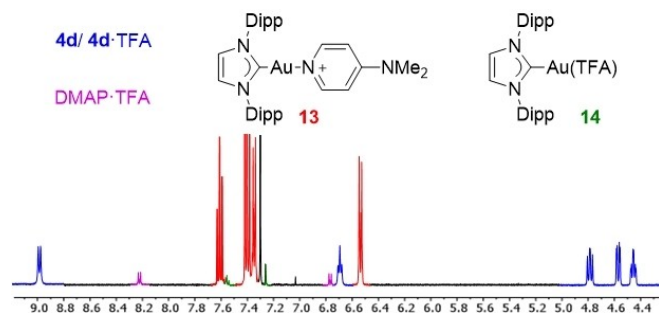
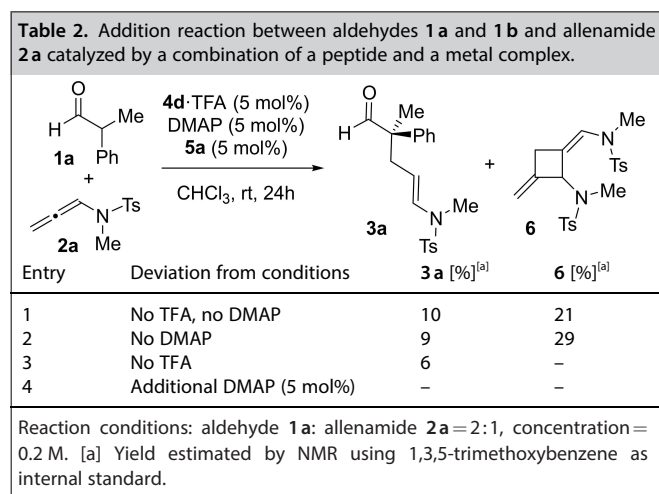


Figure 3. <sup>1</sup>H NMR spectrum of a 1:1:1 mixture of **4d**-TFA, **5a** and DMAP.

**Table 2.** Addition reaction between aldehydes **1a** and **1b** and allenamide **2a** catalyzed by a combination of a peptide and a metal complex.



Entry	Deviation from conditions	<b>3a</b> [%] <sup>[a]</sup>	<b>6</b> [%] <sup>[a]</sup>
1	No TFA, no DMAP	10	21
2	No DMAP	9	29
3	No TFA	6	–
4	Additional DMAP (5 mol%)	–	–

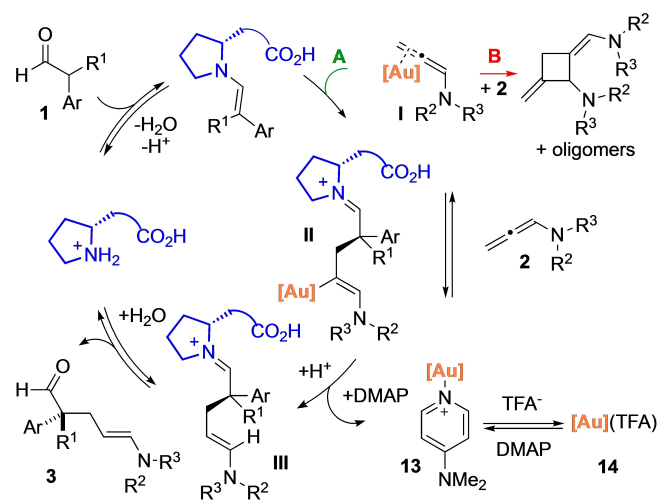
Reaction conditions: aldehyde **1a**: allenamide **2a** = 2:1, concentration = 0.2 M. [a] Yield estimated by NMR using 1,3,5-trimethoxybenzene as internal standard.

(Figures S2–S4).<sup>[17,22]</sup> These experiments demonstrate that an equilibrium exists at the gold center, between the DMAP and TFA ligands. No complexation is, however, observed between the peptide and the gold center in the catalytic mixture. In contrast, a complex mixture was observed between **4d** and **5a** in the absence of DMAP and TFA (Figure S3). Together with the intramolecular salt bridge within the structure of the peptide, these additives thus help to separate the peptide and gold catalysts and disfavor non-productive interactions. These findings suggest that acid and base additives are important for the efficiency of the catalytic reaction.

A series of experiments in which TFA and/or DMAP were excluded or added in excess to the reaction mixture further supported this conclusion (Table 2). In the absence of TFA hardly any product formed and in the absence of DMAP or both additives only small amounts of  $\gamma,\delta$ -enamido aldehyde **3a** formed along with considerable amounts of allenamide dimer **6** (Table 2, entries 1–3). Addition of a two-fold excess of DMAP with respect to the Au-complex and the peptide prevented product formation (Table 2, entry 4) Thus, the absence of DMAP favours dimerization of **2a** to form **6** over reaction to form **3a**. An excess DMAP or the absence of TFA has an inhibitory effect.

These findings support the following catalytic cycle (Scheme 4): The peptide catalyst forms an enamine intermediate with the aldehyde that then reacts in the stereochemistry determining step with an electrophilic  $\pi$ -complex (I) formed through ligand exchange of the Au-DMAP (or Au-TFA) complex with the allenamide. Upon C–C bond formation, vinyl gold-iminium intermediate II is formed, which after protodeauration and hydrolysis furnishes the  $\gamma,\delta$ -enamido aldehyde (**3**) and regenerates the gold and peptide catalysts, respectively.

This mechanistic rationale is in agreement with the observed effects of TFA and DMAP on the reaction. The reduced reaction speed upon increasing the concentration of DMAP likely stems from the equilibrium between the electrophilic  $\pi$ -complex (I) and Au-DMAP complex **13**. The strong coordinating ability of DMAP likely favours gold-complex **13** over intermedi-



Scheme 4. Proposed mechanistic cycle. [Au] = (iPr)Au<sup>+</sup>.

ate I. Increasing the amount of DMAP therefore shifts the equilibrium towards **13** and thus decreases the amount of intermediate I and therefore the overall reaction efficiency. Lowering the concentration of DMAP has the opposite effect, shifting the equilibrium to favour intermediate I. Upon formation of I, two reaction pathways can take place (A (green) and B (red) in Scheme 4). In pathway A, I reacts with the enamine, leading to product **3**. Alternatively, in pathway B, reaction of I with a second equivalent of allenamide **2** takes place, leading to allenamide dimer **6** or higher oligomers. The DMAP thus plays a crucial role in modulating the amount of I, acting to perfectly balance the production of intermediate I, so that pathway A is favoured over other undesired reaction pathways. TFA has a similar effect as increasing its amount should facilitate decomplexation of the DMAP ligand from the gold center by protonation of the pyridine nitrogen. A lower amount of DMAP or a higher amount of TFA should therefore increase the reaction rate. This expectation proved to be correct when performing the reaction with either 3 mol% of DMAP or 7.5 mol% of TFA. In both cases the reaction proceeded faster without sacrificing the enantioselectivity, although with reduced conversion to the  $\gamma,\delta$ -enamido aldehyde (**3a**) (Figure S7).

In summary, we have disclosed the enantioselective addition of branched aldehydes to allenamides, catalyzed by a synergistic combination of a peptide and a gold catalyst. The reaction furnishes  $\alpha$ -alkylated aldehydes bearing either a quaternary or a fully substituted carbon stereogenic center in good to very good enantioselectivities and proceeds under mild conditions. The aldehyde-enamido products can be elaborated into a range of different chiral building blocks including diols, lactones and piperidines. Acid and base additives proved important to control the formation of the electrophilic gold intermediate and its reaction with the enamine intermediate rather than undesired formation of allenamide dimers. Structural modifications as well as in-solution NMR spectroscopic studies showed that the conformational properties of the peptidic catalyst are important for the catalytic efficiency and the selectivity of the reaction. These data demonstrate the robustness and chemoselectivity of peptide catalysts of the type H-Pro-Pro-Xaa, even in increasingly complex environments with metal catalysts. They lay the foundation for the use of peptides in even more complex synergistic catalytic processes, reminiscent of catalytic cascades used by nature.

## Acknowledgements

We thank the European Union's Horizon 2020 research and innovation programme (Grant No 862081) as well as the Swiss National Science Foundation (Grant No 200020\_188729) for financial support and the NMR Service at the Laboratory of Organic Chemistry at ETH Zürich for assistance with the kinetic measurements. Open access funding provided by Eidgenössische Technische Hochschule Zurich.

## Conflict of Interest

The authors declare no conflict of interest.

**Keywords:** asymmetric catalysis · enamides · fully substituted stereogenic centers · gold · peptides

- [1] a) S. Hjorth, S. Waters, N. Waters, J. Tedroff, P. Svensson, A. Fagerberg, M. Edling, B. Svanberg, E. Ljung, J. Gunnergren, S. L. McLean, B. Grayson, N. F. Idris, J. C. Neill, C. Sonesson, *J. Pharmacol. Exp. Ther.* **2020**, JPET-AR-2020-000037; b) K. Rasmussen, D. O. Calligaro, J. F. Czachura, L. J. Dreshfield-Ahmad, D. C. Evans, S. K. Hemrick-Luecke, M. J. Kallman, W. T. Kendrick, J. D. Leander, D. L. Nelson, C. D. Overshiner, D. B. Wainscott, M. C. Wolff, D. T. Wong, T. A. Branchek, J. M. Zgombick, Y.-c. Xu, *J. Pharmacol. Exp. Ther.* **2000**, 294, 688; c) B. Macchia, M. Macchia, A. Martinelli, E. Martinotti, E. Orlandini, F. Romagnoli, R. Scatizzi, *Eur. J. Med. Chem.* **1997**, 32, 231–240; d) A. Cheng, E. Uyeno, W. Polgar, L. Toll, J. A. Lawson, J. I. DeGraw, G. Loew, A. Camerman, N. Camerman, *J. Med. Chem.* **1986**, 29, 531–537.
- [2] For a recent review on enantioselective alkylations of enolates, see: T. B. Wright, P. A. Evans, *Chem. Rev.* **2021**, 121, 9196–9242.
- [3] For reviews on the stereoselective synthesis of quaternary stereogenic centers, see: a) J. Christoffers, A. Baro, *Adv. Synth. Catal.* **2005**, 347, 1473–1482; b) E. J. Corey, A. Guzman-Perez, *Angew. Chem. Int. Ed.* **1998**, 37, 388–401; *Angew. Chem.* **1998**, 110, 402–415; c) C. J. Douglas, L. E. Overman, *Proc. Natl. Acad. Sci. USA* **2004**, 101, 5363; d) K. Fuji, *Chem. Rev.* **1993**, 93, 2037–2066; e) C. Hawner, A. Alexakis, *Chem. Commun.* **2010**, 46, 7295–7306; f) I. Marek, Y. Minko, M. Pasco, T. Mejuch, N. Gilboa, H. Chechik, J. P. Das, *J. Am. Chem. Soc.* **2014**, 136, 2682–2694.
- [4] For examples of the stereoselective synthesis of tertiary ethers, see: a) Y. Uozumi, K. Kato, T. Hayashi, *J. Am. Chem. Soc.* **1997**, 119, 5063–5064; b) B. M. Trost, H. C. Shen, L. Dong, J.-P. Surivet, *J. Am. Chem. Soc.* **2003**, 125, 9276–9277; c) K. Zhang, Q. Peng, X.-L. Hou, Y.-D. Wu, *Angew. Chem. Int. Ed.* **2008**, 47, 1741–1744; *Angew. Chem.* **2008**, 120, 1765–1768; d) S. Tanaka, T. Seki, M. Kitamura, *Angew. Chem. Int. Ed.* **2009**, 48, 8948–8951; *Angew. Chem.* **2009**, 121, 9110–9113; e) J. Xie, W. Guo, A. Cai, E. C. Escudero-Adán, A. W. Kleij, *Org. Lett.* **2017**, 19, 6388–6391; f) K. Shibatomi, M. Kotozaki, N. Sasaki, I. Fujisawa, S. Iwasa, *Chem. Eur. J.* **2015**, 21, 14095–14098; g) D. R. Cefalo, A. F. Kiely, M. Wuchrer, J. Y. Jamieson, R. R. Schrock, A. H. Hoveyda, *J. Am. Chem. Soc.* **2001**, 123, 3139–3140; h) O. A. Wong, Y. Shi, *Chem. Rev.* **2008**, 108, 3958–3987; i) S. E. Denmark, D. J. P. Kornfilt, T. Vogler, *J. Am. Chem. Soc.* **2011**, 133, 15308–15311; j) M. T. Corbett, J. S. Johnson, *Chem. Sci.* **2013**, 4, 2828–2832; k) S.-Y. Zhang, F.-M. Zhang, Y.-Q. Tu, *Chem. Soc. Rev.* **2011**, 40, 1937–1949.
- [5] a) A. R. Brown, W.-H. Kuo, E. N. Jacobsen, *J. Am. Chem. Soc.* **2010**, 132, 9286–9288; b) M. P. Lalonde, Y. Chen, E. N. Jacobsen, *Angew. Chem. Int. Ed.* **2006**, 45, 6366–6370; *Angew. Chem.* **2006**, 118, 6514–6518; c) N. Mase, R. Thayumanavan, F. Tanaka, C. F. Barbas, *Org. Lett.* **2004**, 6, 2527–2530; d) M. R. Witten, E. N. Jacobsen, *Org. Lett.* **2015**, 17, 2772–2775; e) F. Xue, L. Liu, S. Zhang, W. Duan, W. Wang, *Chem. Eur. J.* **2010**, 16, 7979–7982; f) F. Yu, Z. Jin, H. Huang, T. Ye, X. Liang, J. Ye, *Org. Biomol. Chem.* **2010**, 8, 4767–4774; g) A. Quintard, S. Belot, E. Mørchal, A. Alexakis, *Eur. J. Org. Chem.* **2010**, 2010, 927–936; h) B. List, I. Čorić, O. O. Grygorenko, P. S. J. Kaib, I. Komarov, A. Lee, M. Leutzsch, S. Chandra Pan, A. V. Tymtsunik, M. van Gemmeren, *Angew. Chem. Int. Ed.* **2014**, 53, 282–285; *Angew. Chem.* **2014**, 126, 286–289.
- [6] S. Mukherjee, J. W. Yang, S. Hoffmann, B. List, *Chem. Rev.* **2007**, 107, 5471–5569.
- [7] a) Z. Shao, H. Zhang, *Chem. Soc. Rev.* **2009**, 38, 2745–2755; b) Z. Du, Z. Shao, *Chem. Soc. Rev.* **2013**, 42, 1337–1378; c) Y. Deng, S. Kumar, H. Wang, *Chem. Commun.* **2014**, 121, 9196–9242; d) S. Afewerki, A. Córdova, *Chem. Rev.* **2016**, 116, 13512–13570; e) S. Afewerki, A. Córdova, *Top. Curr. Chem.* **2019**, 377, 38;
- [8] For example, see: a) S. Krautwald, D. Sarlah, M. A. Schafroth, E. M. Carreira, *Science* **2013**, 340, 1065; b) X. Mo, D. G. Hall, *J. Am. Chem. Soc.* **2016**, 138, 10762–10765; c) H. Zhou, Y. Wang, L. Zhang, M. Cai, S. Luo, *J. Am. Chem. Soc.* **2017**, 139, 3631–3634; d) F. A. Cruz, V. M. Dong, *J. Am. Chem. Soc.* **2017**, 139, 1029–1032; e) G. Jiang, B. List, *Angew. Chem. Int. Ed.* **2011**, 50, 9471–9474; *Angew. Chem.* **2011**, 123, 9643–9646.

- [9] For reviews on allenamides, see: a) E. Manoni, M. Bandini, *Eur. J. Org. Chem.* **2016**, 3135–3142; b) J. L. Mascareñas, I. Varela, F. López, *Acc. Chem. Res.* **2019**, *52*, 465–479.
- [10] a) D. R. Carbery, *Org. Biomol. Chem.* **2008**, *6*, 3455–3460; b) B. Yang, X. Zhai, S. Feng, D. Hu, Y. Deng, Z. Shao, *Org. Lett.* **2019**, *21*, 330–334; c) X. Yang, F. D. Toste, *Chem. Sci.* **2016**, *7*, 2653–2656.
- [11] a) J. Fernández-Casado, R. Nelson, J. L. Mascareñas, F. López, *Chem. Commun.* **2016**, *52*, 2909–2912; b) A. Ballesteros, P. Morán-Poladura, J. M. González, *Chem. Commun.* **2016**, *52*, 2905–2908.
- [12] C. C. J. Loh, D. Enders, *Chem. Eur. J.* **2012**, *18*, 10212–10225.
- [13] a) M. Wiesner, J. D. Revell, S. Tonazzi, H. Wennemers, *J. Am. Chem. Soc.* **2008**, *130*, 5610–5611; b) M. Wiesner, J. D. Revell, H. Wennemers, *Angew. Chem. Int. Ed.* **2008**, *47*, 1871–1874; *Angew. Chem.* **2008**, *120*, 1897–1900; c) J. Duschmalé, H. Wennemers, *Chem. Eur. J.* **2012**, *18*, 1111–1120; d) R. Kastl, H. Wennemers, *Angew. Chem. Int. Ed.* **2013**, *52*, 7228–7232; *Angew. Chem.* **2013**, *125*, 7369–7373; e) C. E. Grünenfelder, J. K. Kisunzu, H. Wennemers, *Angew. Chem. Int. Ed.* **2016**, *55*, 8571–8574; *Angew. Chem.* **2016**, *128*, 8713–8716; f) T. Schnitzer, H. Wennemers, *J. Am. Chem. Soc.* **2017**, *139*, 15356–15362; g) J. S. Mohler, T. Schnitzer, H. Wennemers, *Chem. Eur. J.* **2020**, *26*, 15623–15628; h) T. Schnitzer, A. Budinska, H. Wennemers, *Nat. Catal.* **2020**, *3*, 143–147.
- [14] For a recent review on peptide catalysis, see: A. J. Metrano, C. R. Shugrue, B. Kim, A. J. Chinn, E. A. Stone, S. J. Miller, *Chem. Rev.* **2020**, *120*, 11479–11615. For tandem reactions of metal and peptide catalysis, see of a) K. Akagawa, T. Fujiwara, S. Sakamoto, K. Kudo, *Org. Lett.* **2010**, *12*, 1804–1807; b) K. Akagawa, T. Fujiwara, S. Sakamoto, K. Kudo, *Chem. Commun.* **2010**, *46*, 8040–8042.
- [15] C. Rigling, J. K. Kisunzu, J. Duschmalé, D. Häussinger, M. Wiesner, M.-O. Ebert, H. Wennemers, *J. Am. Chem. Soc.* **2018**, *140*, 10829–10838.
- [16] S. Suárez-Pantiga, C. Hernández-Díaz, M. Piedrafita, E. Rubio, J. M. González, *Adv. Synth. Catal.* **2012**, *354*, 1651–1657.
- [17] Additional details can be found in the Supporting Information.
- [18] P. de Frémont, E. D. Stevens, M. R. Fructos, M. Mar Díaz-Requejo, P. J. Pérez, S. P. Nolan, *Chem. Commun.* **2006**, 2045–2047.
- [19] For a review on gold catalysis, see: R. Dorel, A. M. Echavarren, *Chem. Rev.* **2015**, *115*, 9028–9072.
- [20] T. Schnitzer, R. L. Ganzoni, H. Wennemers, *Tetrahedron* **2020**, *76*, 131184.
- [21] The use of a prolinolsilyl ether instead of the peptide catalyst provided the product under the same conditions in yields of < 20%, Tables S20 and S21. Of note, previous reports that used prolinolsilyl ethers for the target the reaction used a higher catalyst loading and CH<sub>3</sub>CN or toluene as solvents, solvents that were suboptimal for the catalysis with the peptide **4d**. The results are therefore not directly comparable.
- [22] Deposition Number 2096749 (**3b**), 2096750 (**13**) contain the supplementary crystallographic data for this paper. These data are provided free of charge by the joint Cambridge Crystallographic Data Centre and Fachinformationszentrum Karlsruhe Access Structures service.
- [23] Comparison of the analytical data of the 1,4-diol **7** with that of previously reported data strongly supports that the products formed by the alkyl-aryl aldehydes are (*R*)-configured (see Scheme S1). Note, although the absolute configuration of  $\gamma,\delta$ -enamide aldehydes bearing alkyl versus alkoxy substituents is different following the CIP rules, the relative orientation of the substituents about the fully substituted stereogenic center in both products is the same.

---

Manuscript received: September 3, 2021

Accepted manuscript online: September 8, 2021

Version of record online: October 13, 2021